PHYSICAL REVIEW D **78,** 094011 (2008)

Gravitational and higher-order form factors of the pion in chiral quark models

Wojciech Broniowski[1,2,*] and Enrique Ruiz Arriola[3,+]

[1]*The H. Niewodniczański Institute of Nuclear Physics, Polish Academy of Sciences, PL-31342 Kraków, Poland*
[2]*Institute of Physics, Jan Kochanowski University, PL-25406 Kielce, Poland*
[3]*Departamento de Física Atómica, Molecular y Nuclear, Universidad de Granada, E-18071 Granada, Spain*

(Received 10 September 2008; published 13 November 2008)

The gravitational form factor of the pion is evaluated in two chiral quark models and confronted with the recent full-QCD lattice data. We find good agreement for the case of the spectral quark model, which builds in the vector-meson dominance for the charge form factor. We derive a simple relation between the gravitational and electromagnetic form factors, holding in the considered quark models in the chiral limit. The relation implies that the gravitational mean squared radius is half the electromagnetic one. We also analyze higher-order quark generalized form factors of the pion, related to higher moments in the symmetric Bjorken X variable of the generalized parton distribution functions, and discuss their perturbative QCD evolution, which is needed to relate the quark-model predictions to the lattice data. The values of the higher-order quark form factors at $t = 0$, computed on the lattice, also agree with our quark-model results within the statistical and method uncertainties.

DOI: 10.1103/PhysRevD.78.094011 PACS numbers: 12.38.Lg

I. INTRODUCTION

Form factors carry basic information on the extended structure of hadrons, as they correspond to matrix elements of conserved currents between hadron states. There exist abundant experimental data concerning the charge form factor, which is related to the electromagnetic current and provides the distribution of charge in a hadron. The *gravitational form factors*, which are related to matrix elements of the energy-momentum tensor [1] in a hadronic state and thus provide the distribution of matter within a hadron, are not experimentally known. This is because, whereas the electromagnetic interactions are probed by structureless electrons and mediated by one-photon exchange, the parallel one-graviton exchange is extremely weak and impossible to measure. Recently, however, these objects were determined *ab initio* and with sufficient accuracy in full-QCD lattice simulations by the QCDSF/UKQCD Collaboration [2,3]. In this paper we confront the predictions of chiral quark models for the pion gravitational form factors and higher-order generalized form factors with the lattice determination of Refs. [2,3]. We find that in the spectral quark model (SQM) [4], which is a variant of a chiral quark model with built-in vector meson dominance, the agreement with the lattice data is especially good. In particular, a slower falloff with the large spacelike momenta than for the case of the electromagnetic form factor is found. We also perform the calculations in the Nambu–Jona-Lasinio (NJL) model with the Pauli-Villars (PV) regularization, where the agreement is not as good as in the SQM. In addition, we find that the higher-order generalized form factors (see below for a definition) at $t = 0$ provided by the full-QCD lattice simulations are properly reproduced in chiral quark models.

The form factors are related via sum rules to more general objects, the generalized parton distributions (GPDs) of the pion (for extensive reviews see e.g. [5–13] and references therein). Experimentally, the GPDs of the pion are elusive quantities, as they appear in exclusive processes which are difficult to measure, such as the deeply virtual Compton scattering or the hard electroproduction of mesons. Recently, it has been suggested to study instead the deeply virtual Compton scattering on a virtual pion that is emitted by a proton [14] under the operating conditions which will first be met after the energy upgrade at TJLAB. This will eventually set important constraints on the pion GPDs.

Despite their fundamental and general character, GPDs are genuinely defined in Minkowski space, thus hindering direct determinations on Euclidean lattices. The moments of GPDs in the X variable (see Sec. II) form polynomials in the ξ variable, with coefficients depending on the t variable only. The lowest moments yield the standard electromagnetic and the gravitational form factors, while higher moments are known as *generalized form factors*. These are useful quantities which may be computed directly on the lattice. Presently, apart from the values at $t = 0$, the generalized form factors are not known even from lattice simulations due to insufficient statistics. In this work we make predictions for the first few generalized form factors. Since these objects do not correspond to conserved currents, they evolve with the QCD scale as they carry anomalous dimensions. We undertake this perturbative analysis at leading order and show how the generalized form factors evolve with the scale. We use the techniques described in detail in Ref. [15].

*Wojciech.Broniowski@ifj.edu.pl
+earriola@ugr.es

Chiral quark models have proved to properly describe the essential features of the pionic GPDs and related quantities. The special case of the parton distribution function (PDF) has been analyzed in the NJL model in Refs. [16–18]. The diagonal GPD in the impact parameter space was obtained in [19]. Other calculations of the pionic GPDs and PDFs were performed in instanton-inspired chiral quark models [20–27]. In the effective quark models the GPDs have been analyzed in [15,21,28–30]. Studies paying particular attention to polynomiality were carried out in [21,31,32], which proceeded via double distributions [33]. The same technique was applied in Ref. [15], which allowed for a simple proof of polynomiality in chiral quark models. Also, other formal features, such as support, normalization, crossing, and the positivity constraints [34,35], were all satisfied in the chiral quark-model calculation of Ref. [15]. Moreover, the obtained analytic expressions have a rather nontrivial form which is not factorizable in the t variable. The parton distribution amplitude (PDA), related to the GPD via a low-energy theorem [36], was evaluated in Refs. [37–41] (see Ref. [42] for a brief review of the analyses of PDA). The authors of Ref. [14] provide standard electromagnetic and gravitational form factors based on a phenomenological model factorization assumption which is generally not satisfied by our dynamical field-theoretical calculation [15]. Finally, the related quantity, the pion-photon transition distribution amplitude (TDA) [43–46], has been obtained in Refs. [47–51].

In the present work we find that in the considered class of models a simple relation between the gravitational and charge form factors holds (see the Appendix). The essential element for the proof is the existence of the spectral representation of the quark model, which is the case both for SQM and NJL with the Pauli-Villars regularization. The relation implies that in the considered models and in the chiral limit the gravitational mean squared radius is half the electromagnetic one.

In Ref. [15] we have stressed the relevance of the QCD evolution for the phenomenological success of the chiral quark models in the description of the experimental and lattice data for the PDF and PDA of the pion. Indeed, the evolved results for the valence PDF compare very well to the Drell-Yan data from the E615 experiment [52] at the scale of 4 GeV, and to the transverse lattice results [53] at lower scales, ~0.5 GeV. Similarly, for the case of the PDA the QCD evolution leads to a fair description of the E791 dijet data [54] at the scale of 2 GeV, and of the transverse lattice data [53] at the lattice scale. The comparison is presented in Figs. 8–11 of Ref. [15].

The above-mentioned success of the chiral quark models in describing properties related to the pionic GPD allows us to hope that their other aspects, such as the form factors, including the generalized ones, can also be reliably estimated in these models. Certainly, the electromagnetic form factor, as one of the most basic quantities, has been promptly computed in all chiral quark models of the pion. Note that these evaluations assume the large-N_c limit; thus the effects of the pion loops, important at low momenta, are absent. We note that the NJL model leads to a somewhat too small electromagnetic radius [41], while in SQM, which incorporates the vector meson dominance, one may fit the data accurately. Some predictions of the NJL model for the generalized form factors of the pion have been presented by one of us in Ref. [55]; however, the data away from the physical pion mass have been used in that work.

The outline of the paper is as follows: In Sec. II we review the necessary formalism, providing basic definitions and notation. The essential information on the two chiral quark models used in our work is provided in Sec. III, while Sec. IV shows their predictions for the electromagnetic and gravitational form factors. In Sec. V, which contains our main results, we compare our predictions to the full-QCD lattice data from Refs. [2,3]. Then, in Sec. VI we give the results for the higher-order form factors, where the QCD evolution effects are incorporated.

II. BASIC DEFINITIONS

In this section we review the basic concepts necessary for our analysis and introduce the notation.

Throughout this paper we work, for simplicity, in the strict chiral limit,

$$m_\pi = 0. \tag{1}$$

Since the lattice data of Refs. [2,3] give the extrapolation to the physical pion mass which is small, the assumption (1) is appropriate. Nevertheless, the extension to the physical pion mass in chiral quark models is straightforward. In any case, it is worth mentioning that, although an attempt was made [2,3] to incorporate chiral logarithms from chiral perturbation theory (χPT) to the one-loop order [56–58] (for a review see e.g. Ref. [59]), as described in Ref. [60], the data did not exhibit their presence when all other uncertainties were considered, suggesting instead a linear extrapolation.

In this paper we will deal with standard gravitational and vector form factors. The corresponding quark operators are

$$\Theta^{\mu\nu} = \sum_{q=u,d,\ldots} \bar{q}(x)\frac{\mathrm{i}}{2}(\gamma^\mu\partial^\nu + \gamma^\nu\partial^\mu)q(x) \tag{2}$$

and

$$J_V^\mu = \sum_{q=u,d,\ldots} \bar{q}(x)\frac{\tau_a}{2}\gamma^\mu q(x), \tag{3}$$

respectively. The gravitational quark form factors of the pion [61], Θ_1 and Θ_2, are defined through the matrix element of the energy-momentum tensor in the one-pion state,

$$\langle \pi^b(p') \mid \Theta^{\mu\nu}(0) \mid \pi^a(p)\rangle = \tfrac{1}{2}\delta^{ab}[(g^{\mu\nu}q^2 - q^\mu q^\nu)\Theta_1(q^2) + 4P^\mu P^\nu \Theta_2(q^2)], \quad (4)$$

where $P = \frac{1}{2}(p' + p)$, $q = p' - p$, and a, b are the isospin indices. The gravitational form factors satisfy the low-energy theorem $\Theta_1(0) - \Theta_2(0) = \mathcal{O}(m_\pi^2)$ [61]. In the low-momentum and pion-mass limit one can establish contact with χPT in the presence of gravity [61],

$$\Theta_1(q^2) = 1 + \frac{2q^2}{f^2}(4L_{11} + L_{12}) - \frac{16m^2}{f^2}(L_{11} - L_{13}) + \ldots, \quad (5)$$
$$\Theta_2(q^2) = 1 - \frac{2q^2}{f^2}L_{12} + \ldots,$$

where $f = 86$ MeV is the pion weak decay constant in the chiral limit and $L_{11,12,13}$ are the corresponding gravitational low-energy constants. The calculation of the effective energy-momentum tensor as well as the low-energy constants for chiral quark models has been carried out in Refs. [62,63]. The vector form factor is defined as

$$\langle \pi^a(p')|J_V^{\mu,b}(0)|\pi^c(p)\rangle = \epsilon^{abc}(p'^\mu + p^\mu)F_V(q^2). \quad (6)$$

At low momentum one has

$$F_V(q^2) = 1 + \frac{2q^2L_9}{f^2} + \ldots \quad (7)$$

where L_9 is a low-energy constant of χPT [58].

The generalized quark form factors of the pion (here we take π^+ for definiteness) are defined as matrix elements of quark bilinears accompanied by additional derivative operators,

$$\langle \pi^+(p')|\bar{u}(0)\gamma^{\{\mu}i\overleftrightarrow{D}^{\mu_1}i\overleftrightarrow{D}^{\mu_2}\ldots i\overleftrightarrow{D}^{\mu_{n-1}\}}u(0)|\pi^+(p)\rangle = 2P^{\{\mu}P^{\mu_1}\ldots P^{\mu_{n-1}\}}A_{n0}(t) + 2\sum_{k=2\text{ even}}^{n} q^{\{\mu}q^{\mu_1}\ldots q^{\mu_{k-1}}P^{\mu_k}\ldots P^{\mu_{n-1}\}}2^{-k}A_{nk}(t), \quad (8)$$

where $A_{nk}(t)$ are the generalized form factors with $n = 1, 2, \ldots$ and $k = 0, 2, \ldots, n$. The symbol $\vec{D}$ is the QCD covariant derivative, $\overleftrightarrow{D} = \frac{1}{2}(\vec{D} - \overleftarrow{D})$, and $\{\ldots\}$ denotes the symmetrization of indices and the subtraction of traces for each pair of indices. The factor of 2^{-k} is conventional and makes our definition different than in Refs. [2,3]. For $n = 1$ and 2 we have

$$A_{10}(t) = F_V(t), \qquad A_{20}(t) = \tfrac{1}{2}\Theta_1^q(t), \qquad A_{22}(t) = -\tfrac{1}{2}\Theta_2^q(t), \quad (9)$$

where F_V is the pion electromagnetic form factor, while Θ_i^q denote the quark parts of the gravitational form factors of Eq. (8).

Chiral quark models work at the scale where the only explicit degrees of freedom are quarks, while the gluons are integrated out. Thus, the gluon form factors of the pion vanish,

$$A_{nk}^G(t) = 0 \qquad \text{(quark-model scale)}. \quad (10)$$

When evolution to higher scales is carried out [15], nonzero gluonic moments are generated. Note that the above-mentioned soft-pion theorem $\Theta_1(0) = \Theta_2(0) + \mathcal{O}(m_\pi^2)$ applies to the *full* trace of the energy-momentum tensor and, consequently, does not apply to its quark or gluonic contributions separately. The condition (10) then translates into $A_{20}(0) = -A_{22}(0)$ in the chiral limit at the quark-model scale.

Now we pass to the definition of the GPDs, whose moments are related to the form factors listed above. The conventions used are the same as in Ref. [15], where all the details of the calculation of the GPDs can also be found. The kinematics of the GPDs can be read off from Fig. 1. The adopted notation is

$$p^2 = m_\pi^2 = 0, \qquad q^2 = -Q^2 = -2p\cdot q = t, \qquad n^2 = 0, \qquad p\cdot n = 1, \qquad q\cdot n = -\zeta, \quad (11)$$

with the null vector n defining the light cone. The two isospin projections of the quark GPDs of the pion, isosinglet (singlet) and isovector (nonsinglet), are defined through the matrix elements of quark bilinears, with the quark fields displaced along the light cone,

$$\delta_{ab}\mathcal{H}^{I=0}(x,\zeta,t) = \int \frac{dz^-}{4\pi}e^{ixp^+z^-}\langle \pi^b(p+q)|\bar{\psi}(0)\gamma \cdot n\psi(z)|\pi^a(p)\rangle|_{z^+=0,z^\perp=0}, \quad (12)$$

$$i\epsilon_{3ab}\mathcal{H}^{I=1}(x,\zeta,t) = \int \frac{dz^-}{4\pi}e^{ixp^+z^-}\langle \pi^b(p+q)|\bar{\psi}(0)\gamma \cdot n\psi(z)\tau_3|\pi^a(p)\rangle|_{z^+=0,z^\perp=0}. \quad (13)$$

The coordinate z lies on the light cone. At the quark-model scale the gluon GPD of the pion vanishes,

$$\mathcal{H}^G(x,\zeta,t) = 0 \qquad \text{(quark-model scale)}. \quad (14)$$

When the QCD evolution to higher scales is performed, a nonvanishing gluonic contribution $\mathcal{H}^G(x,\zeta,t)$ is generated [15].

In the following analysis we use the *symmetric* notation for the GPDs,

$$\xi = \frac{\zeta}{2-\zeta}, \qquad X = \frac{x-\zeta/2}{1-\zeta/2}, \quad (15)$$

where $0 \le \xi \le 1$ and the support is $-1 \le X \le 1$. One introduces the corresponding GPDs,

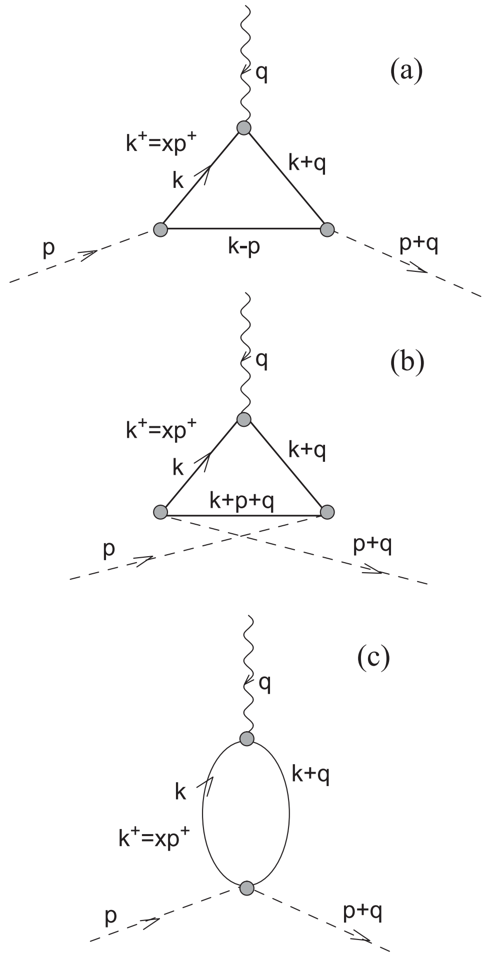

FIG. 1. The direct (a), crossed (b), and contact (c) Feynman diagrams for the quark-model evaluation of the GPD of the pion. The contact contribution is responsible for the D-term.

$$H^{I=0,1}(X,\xi,t) = \mathcal{H}^{I=0,1}\left(\frac{\xi+X}{\xi+1},\frac{2\xi}{\xi+1},t\right). \quad (16)$$

The reflection about $X=0$ yields the symmetry relations

$$H^{I=0}(X,\xi,t) = -H^{I=0}(-X,\xi,t),\ H^{I=1}(X,\xi,t) = H^{I=1}(-X,\xi,t). \quad (17)$$

At $X \geq 0$ the GPDs are related to the PDF, $q(X)$,

$$H^{I=0}(X,0,0) = H^{I=1}(X,0,0) = q(X).$$

The *polynomiality* conditions [5,6] follow from very basic field-theoretic assumptions, namely, the Lorentz invariance, time reversal, and Hermiticity, which yield the form (8). For the moments one finds

$$\int_{-1}^{1} dX X^{2j} H^{I=1}(X,\xi,t) = 2\sum_{i=0}^{j} A_{2j+1,2i}(t)\xi^{2i},$$
$$\int_{-1}^{1} dX X^{2j+1} H^{I=0}(X,\xi,t) = 2\sum_{i=0}^{j+1} A_{2j+2,2i}(t)\xi^{2i}, \quad (18)$$

with $j = 0, 1, \ldots$. For the lowest moments one has

$$\int_{-1}^{1} dX H^{I=1}(X,\xi,t) = 2A_{10}(t) = 2F_V(t), \quad (19)$$

$$\int_{-1}^{1} dX X H^{I=0}(X,\xi,t) = 2A_{20}(t) + 2A_{22}(t)\xi^2 = \Theta_2(t) - \Theta_1(t)\xi^2. \quad (20)$$

In the convention of Refs. [2,3] the equivalent expansion is in powers of $(2\xi)^2$ rather than ξ^2, as in Eq. (18). In our approach, used in the following sections, polynomiality is explicitly manifest from the use of the double distributions [15]. The equivalence of Eqs. (8) and (18) is easily proven by contracting (8) with the null vectors $n^{\mu_1}\ldots n^{\mu_j}$ and subsequently applying the definitions (11). We notice that for the isovector GPD only the even moments are nonvanishing, and for the isoscalar GPD only the odd moments are nonvanishing. The gluon form factors are defined as the integrals

$$\int_{-1}^{1} dX X^{2j+1} H_g(X,\xi,t,Q^2) = 2\sum_{i=0}^{j+1} A^G_{2j+2,2i}(t)\xi^{2i}. \quad (21)$$

Finally, we note that Eq. (18) for $j=0$ expresses the electric charge conservation and the momentum sum rule operating in deep inelastic scattering.

III. CHIRAL QUARK MODELS

In chiral quark models at the leading-N_c level the calculation of the form factors and GPDs proceeds according to the one-loop diagrams of Fig. 1. Extensive details of the quark-model evaluation are given in [15]. In this paper we carry out calculations in two chiral quark models: SQM [4] and NJL with the Pauli-Villars regularization in the twice-subtracted version of Refs. [41,64,65]. Variants of chiral quark models differ in the way they perform the necessary regularization of the quark loop diagrams.

The spectral quark model [4] introduces the generalized spectral density $\rho(\omega)$ in the quark mass ω, in the spirit of Ref. [66], supplied with chiral symmetry, gauge invariance, and vector meson dominance. The one-quark-loop action of the SQM has the form

$$\Gamma_{\rm SQM} = -iN_c \int_C d\omega \rho(\omega)\,{\rm Tr}\log(i\partial\!\!\!/ - \omega U^5), \quad (22)$$

where $\rho(\omega)$ is the quark generalized *spectral function*, and $U^5 = \exp(i\gamma_5 \boldsymbol{\tau}\cdot\boldsymbol{\phi}/f)$, with $\boldsymbol{\phi}$ denoting the pion field in the nonlinear realization. The vector part of the spectral function, needed in the present analysis, has the vector-meson-dominance form [4]

$$\rho_V(\omega) = \frac{1}{2\pi i}\frac{1}{\omega}\frac{1}{(1-4\omega^2/m_\rho^2)^{5/2}}, \quad (23)$$

exhibiting the pole at the origin and cuts starting at

$\pm m_\rho/2$, where $m_\rho \sim 770$ MeV is the mass of the rho meson. The complex contour C for the integration in (22) is given in Ref. [4]. The SQM leads to conventional and successful phenomenology for the pion [4,15,62,67], the nucleon [68], and the photon parton distribution amplitude [69].

We also study a more conventional chiral quark model, the NJL model with the Pauli-Villars regularization in the twice-subtracted version proposed in Refs. [41,64,65]. The one-quark-loop action of the model is

$$\Gamma_{\rm NJL} = -iN_c \,{\rm Tr} \log(i\not{\partial} - MU^5), \tag{24}$$

where M is the constituent quark mass. The Pauli-Villars regularization is introduced at the effective action level [41,64,65], with the practical advantage that gauge and relativistic symmetries as well as sum rules are manifestly fulfilled [70]. For the observables considered in this paper, the Pauli-Villars regularization is implemented according to the prescription where instances of M^2 in an observable $\mathcal{O}$ are replaced with $M^2 + \Lambda^2$, and then the regularized observable is evaluated according to the prescription

$$\mathcal{O}_{\rm reg} = \mathcal{O}(0) - \mathcal{O}(\Lambda^2) + \Lambda^2 \frac{d\mathcal{O}(\Lambda^2)}{d\Lambda^2}. \tag{25}$$

The Pauli-Villars regulator Λ is a free parameter of the model. In what follows we use

$$M = 280 \text{ MeV}, \qquad \Lambda = 871 \text{ MeV}, \tag{26}$$

which yields $f = 93.3$ MeV for the pion decay constant [41] according to the formula

$$f^2 = -\frac{N_c M^2}{4\pi^2}[\log(\Lambda^2 + M^2)]_{\rm reg}. \tag{27}$$

IV. ELECTROMAGNETIC AND GRAVITATIONAL FORM FACTORS

The form factors may be calculated in two different ways. The first method uses the definition (8), which leads to the evaluation of one-loop diagrams with an appropriate vertex. For the electromagnetic form factor the vertex is $Q\gamma^\mu$, where Q is the electric charge of the quark. For the gravitational form factor the vertex, corresponding to the energy-momentum tensor, has the form

$$\Theta^{\mu\nu}(k+q,k) = \tfrac{1}{4}[(2k+q)^\mu\gamma^\nu + (2k+q)^\nu\gamma^\mu] - \tfrac{1}{2}g^{\mu\nu}(2\not{k} + \not{q} - \omega), \tag{28}$$

with ω denoting the quark mass. We illustrate the calculation in the Appendix. The other method uses the GPDs obtained earlier [15] and evaluates their moments (18). The results are the same, which serves as a consistency test of the algebra. As mentioned in Sec. II, the equivalence is proven by contracting with the null vector. For instance, in the case of the gravitational form factor, we consider $n_\mu \Theta^{\mu\nu} n_\nu$. Then

$$\langle \pi^b(p+q) \mid n_\mu \Theta^{\mu\nu}(0) n_\nu \mid \pi^a(p)\rangle = \delta^{ab}\tfrac{1}{2}[\zeta^2\Theta_1(q^2) + (2-\zeta)^2\Theta_2(q^2)] \tag{29}$$

and the vertex becomes

$$n_\mu \Theta^{\mu\nu}(k+q,k) n_\nu = (x - \zeta/2)\gamma\cdot n. \tag{30}$$

We recognize the same vertex as in the evaluation of the GPDs multiplied by $(x-\zeta/2)$. Upon passing to the symmetric notation, Eq. (20) follows.

Before showing the explicit results both for SQM and NJL models in the specific realizations described in the previous section, we note some general results. Actually, in the considered quark models and in the chiral limit, we have the following identity relating the gravitational and electromagnetic form factors,

$$\frac{d}{dt}[t\Theta_i(t)] = F_V(t) \qquad (i = 1, 2), \tag{31}$$

from which the identity between the two gravitational form factors $\Theta_1(t) = \Theta_2(t) \equiv \Theta(t)$ follows. These remarkable quark-model relations are proven explicitly in the Appendix. The essential ingredient of the proof is the existence of the spectral representation in both considered models. One consequence of relation (31) is the expected consistency of normalizations at $t = 0$ for the charge and mass $\Theta_i(0) = F_V(0)$, displaying the tight connection between the gauge and Poincare invariances. Furthermore, expanding in small t and using the fact that $F(t) = F(0) \times [1 - \langle r^2\rangle t/6 + \ldots]$ with $\langle r^2\rangle$ denoting the mean squared radius, one gets

$$2\langle r^2\rangle_\Theta = \langle r^2\rangle_V, \tag{32}$$

which means that in the considered models and in the chiral limit the gravitational mean squared radius is half the electromagnetic one.

Turning now to the specific realization, by construction, the pion electromagnetic form factor in the SQM has the monopole form

$$F_V^{\rm SQM}(t) = \frac{m_\rho^2}{m_\rho^2 - t}. \tag{33}$$

A straightforward evaluation for the gravitational form factor yields

$$\Theta_1^{\rm SQM}(t) = \Theta_2^{\rm SQM}(t) = \frac{m_\rho^2}{t}\log\left(\frac{m_\rho^2}{m_\rho^2 - t}\right) \equiv \Theta^{\rm SQM}(t). \tag{34}$$

These specific form factors fulfill trivially the general relations Eqs. (31) and (32).

In the NJL model the pion electromagnetic form factor is equal to

$$F_V^{\rm NJL}(t) = 1 + \frac{N_c g_\pi^2}{8\pi^2}\left(\frac{2s\log(\frac{s-\sqrt{-t}}{s+\sqrt{-t}})}{\sqrt{-t}}\right)_{\rm reg},$$

with $g_\pi = M/f$ denoting the quark-pion coupling constant. We have introduced the shorthand notation $s = \sqrt{4(M^2+\Lambda^2)-t}$. The condition $\lim_{t\to-\infty} F_{\rm NJL}(t) = 0$ is satisfied due to Eq. (27). For the gravitational form factor we obtain

$$\Theta^{\rm NJL}(t) = F_V^{\rm NJL}(t) - \frac{N_c g_\pi^2}{8\pi^2}\left(\frac{4(M^2+\Lambda^2)}{t}\left[\mathrm{Li}_2\left(\frac{2\sqrt{-t}}{s+\sqrt{-t}}\right) + \mathrm{Li}_2\left(\frac{2\sqrt{-t}}{\sqrt{-t}-s}\right)\right]\right)_{\rm reg}, \quad (35)$$

where $\mathrm{Li}_2(z)$ is the polylogarithm function.

Of course, the explicit expressions (33)–(35) comply with the general relation (31).

Similar expressions, of growing complication, may be obtained for higher-order form factors in both SQM and NJL models.

V. COMPARISON TO THE LATTICE DATA

We are now ready to compare the results of the previous section to the recent lattice data [2,3]. These data correspond to the scale of $Q = 2$ GeV and give the quark part of the gravitational form factor and the electromagnetic form factor. On the other hand, the quark-model calculation corresponds to a very low scale, $Q_0 \sim 320$ MeV, and, in general, the QCD evolution is needed to compare the model predictions to the data at a different scale Q.

A detailed discussion of the evolution issue is presented in Ref. [15]. The low-energy chiral quark models contain *quarks* as the basic and explicit degrees of freedom, and the considered twist-2 observables correspond to modeling QCD at a low renormalization point. Obviously, by the energy-momentum conservation in these models, the quarks as the only degrees of freedom carry 100% of the total momentum in a hadron. On the other hand, the momentum fraction carried by the valence quarks in the pion at the scale $Q^2 = 4$ GeV^2 is about 40%. The QCD evolution [LO, next-to-leading order (NLO), next-to-next-to leading order] tells us that this number grows as the scale is evolved to *lower values*. The quark-model reference scale Q_0 is determined as the scale where the evolved QCD value yields exactly the inescapable 100% of the quark model. It would of course be highly desirable to include, e.g., explicit gluonic degrees of freedom, as this would allow one to stop the perturbative evolution at a higher scale. Nonetheless, the LO and NLO evolutions for the PDFs are sufficiently close to each other [18] as to provide some confidence in the kind of calculations carried out in our work.

The issue of the QCD evolution of GPDs and the generalized form factors is addressed in detail in Sec. VI. However, the electromagnetic and gravitational form factors do not evolve with the scale. What changes is the ratio R of the total momentum fraction carried by the quarks (valence and sea),

$$R = \frac{\langle x\rangle_q(Q)}{\langle x\rangle_q(Q_0)} = \left(\frac{\alpha(Q)}{\alpha(Q_0)}\right)^{\gamma_1^{(0)}/(2\beta_0)}, \quad (36)$$

where the anomalous dimension is given by $\gamma_1^{(0)}/(2\beta_0) = 32/81$ for $N_F = N_c = 3$ and

$$\alpha(Q^2) = \frac{4\pi}{\beta_0 \log(Q^2/\Lambda_{\rm QCD}^2)}, \quad (37)$$

$$\beta_0 = \frac{11}{3}N_c - \frac{2}{3}N_f, \quad (38)$$

where we take $\Lambda_{\rm QCD} = 226$ MeV and $N_c = N_f = 3$. At the scale Q_0 we have $R = 1$, which then gradually decreases with the increasing scale. The quark part of the gravitational form factor is $\Theta^q(t) = R\Theta(t)$, and the gluon part is $\Theta^G(t) = (1-R)\Theta(t)$, such that, of course, $\Theta^q(t) + \Theta^G(t) = \Theta(t)$.

The value of R depends on the evolution ratio $\alpha(Q^2)/\alpha(Q_0^2)$, which is not precisely known on the lattice. For that reason we shall treat R as a free parameter when fitting the model results to the data for the gravitational form factor. In the SQM the other parameter is the value of the rho meson mass, m_ρ. For the SQM we fit jointly the electromagnetic part and the quark part of the gravitational form factor. The χ^2 method yields

$$R = 0.28 \pm 0.02, \qquad m_\rho = 0.75 \pm 0.05 \text{ GeV}, \quad (39)$$

with $\chi^2/\mathrm{DOF} = 1.8$. The result of the fit is displayed in Fig. 2 with the solid line. The band corresponds to the uncertainties in the values of the parameters in Eq. (39). We note an overall very good agreement for both form factors. Note that there is a significantly slower falloff for the gravitational form factor compared to the electromagnetic one. The optimum value of m_ρ agrees within the error bars, which are substantial, with the physical mass of the rho meson.

For the case of the NJL model (dashed line in Fig. 2) the agreement is not as good as in the SQM model and it is not possible to improve it by changing the parameters M and Λ. For that reason we have not carried out the χ^2 fit in this case. The problems of the NJL model in reproducing the electromagnetic form factor, where the corresponding rms radius turns out to be too small, are well known; see e.g. the discussion in Ref. [41]. A similar discrepancy can be noted for the case of the gravitational form factor shown in the bottom panel of Fig. 2.

Now we come back, in greater detail, to the issue of the quark to gluon momentum ratio R. It evolves with the scale from the value $R = 1$ at the quark-model scale to $R \to 0$ at $Q^2 \to \infty$. We use the standard LO Dokshitzer-Gribov-Lipatov-Altarelli-Parisi (DGLAP) evolution for the single channel. We know the final scale, $Q = 2$ GeV, but the quark-model scale is *a priori* unknown. We thus adjust Q_0 in order to reach the value of R from Eq. (39) at the known scale Q. The result is

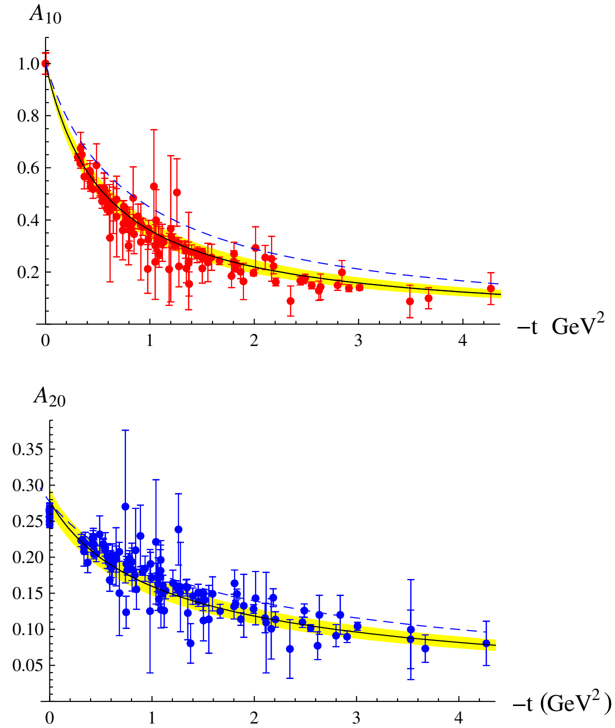

FIG. 2 (color online). The electromagnetic form factor (top panel) and the quark part of the gravitational form factor (bottom panel) in the SQM (solid line) and the NJL model (dashed line) compared to the lattice data from Ref. [3]. The band around the SQM results corresponds to the uncertainty in the quark momentum fraction R and the m_ρ parameter.

$$Q_0 = 0.31 \pm 0.03 \text{ GeV} \tag{40}$$

with $\Lambda_{\rm QCD} = 226$ MeV. This value agrees with the earlier independent determinations of the quark-model scale; see Ref. [15] for a detailed discussion on these issues. We note that at such low scales as in Eq. (40) the perturbative expansion parameter in the DGLAP equations is large, $\alpha(Q_0^2)/(2\pi) = 0.34$, which makes the evolution very fast for the scales in the vicinity of Q_0.

One should note that the large value of $\alpha(Q_0^2)$ calls for the use of improved QCD evolution at low scales. The presented analysis could be extended in several ways, for instance, incorporating the NLO effects, or by modifying the dependence of α on Q^2 at low scales, incorporating the "infrared protection" [71]. The NLO corrections to the meson PDFs in chiral quark models were studied in Ref. [18], where, somewhat surprisingly, it was found that these effects are small. Modifications in the evolution of $\alpha(Q^2)$ could be incorporated along the lines of Refs. [72–74] where they were used for the pion form factor, but this calculation is outside the scope of the present paper.

We stress that the chiral quark-model explanation of the lattice data used in this work as well as the physical and lattice data explored in Ref. [15] requires "strong" evolution, with a large value of the evolution ratio $\alpha(Q_0^2)/\alpha(Q^2)$. Our simpleminded analysis based on the LO evolution may be viewed as an approximation to a more elaborate scheme; nevertheless, it is quite remarkable that various observables (PDFs, PDAs, their moments) lead to the same evolution ratio, giving, in the LO approximation, compatible quark-model scales [15]. Moreover, the electromagnetic and the gravitational form factors are independent of the evolution; hence the issue does not arise for these observables.

In Fig. 3 we show the form factor multiplied by $-t$, which is a popular way to present the results at large Euclidean momenta. In the case of the vector (electromagnetic) form factor we also display the experimental TJLAB data [75–77] and the earlier Cornell data [78], and the approximately constant value for $-tF_V(t)$ is clearly seen. In the gravitational case, however, the lattice data [2,3] show an increasing trend which is well mimicked by our SQM form factor, $-t\Theta(t) \sim \log(-t)$.

In the large-N_c limit in the single resonance approximation (SRA) [61,79], one would have a monopole form factor

$$\Theta^{\rm SRA}(t) = \frac{AM_f^2}{M_f^2 - t}, \tag{41}$$

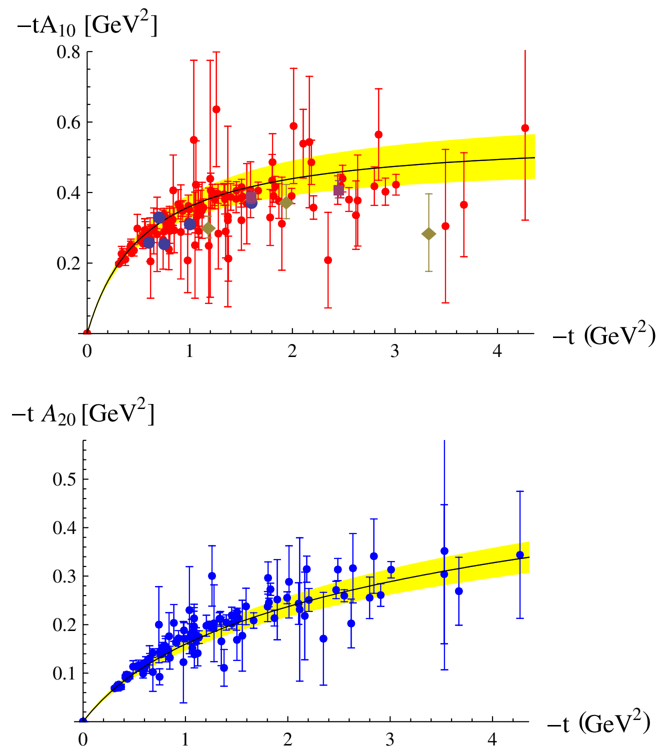

FIG. 3 (color online). Same as Fig. 2 for the form factors multiplied with $-t$. In addition, we include the TJLAB data [75–77] (darker and larger circles and squares) and the Cornell data [78] (diamonds).

which agrees with our quark model at low t if $M_f = \sqrt{2}M_V \sim 1100$ MeV, in agreement with the result of Eq. (32). The difference between the SRA form factor and our Eq. (34) is less than 10% for momentum values up to $t = -1\ \mathrm{GeV}^2$. The SRA monopole fits well the data extrapolated to the physical pion mass, yielding $A = 0.261(5)$ and $M_f = 1320(60)$ MeV [2,3].

To conclude this section, several general remarks are in order. One has to bear in mind that the full-QCD lattice calculations are linearly extrapolated to the physical pion mass. Our quark-model analysis incorporates only the leading-N_c contributions, while the full-QCD simulations include all orders in that expansion. Nevertheless, despite these caveats, we note a quite remarkable agreement, in particular for the case of the SQM. This is noteworthy, as our study is a genuine dynamical field-theoretical calculation, and the parameters providing the optimal fit are highly compatible with calculations of other processes within the *same model and scheme*.

Admittedly, at very large values of $-t$, perturbative QCD results for the form factors should be reached. At very low values of t, chiral corrections are important. Since the data we use are at intermediate values of Euclidean momenta, we may neglect both the above-mentioned effects and use the chiral quark models to explain the data.

We stress that our calculation conforms to the low-energy theorem $\Theta_1(0) - \Theta_2(0) = \mathcal{O}(m_\pi^2)$ [61], which is dictated by chiral symmetry. The quark model predicts, in addition, $\Theta_1(t) = \Theta_2(t)$, and the purely multiplicative character of the QCD evolution yields, in our conventions,

$$A_{22}(t) = -A_{20}(t). \tag{42}$$

Probably due to insufficient statistics, this formula is not quite seen in the data of Ref. [3] [note that with conventions adopted in that reference one should have instead $A_{22}(t) = -\frac{1}{4}A_{20}(t)$]. For that reason we have not used the data for A_{22} in our numerical analysis.

VI. HIGHER-ORDER FORM FACTORS

Analogous calculations as in the previous section can be performed for the higher-order generalized form factors. Here we only give the results for the case of the SQM, as the results in NJL are qualitatively similar, and also the SQM works better for those quantities which can be confronted with the data. In Fig. 4(a) we show $A_{3,2i}$ and $A_{4,2i}$ obtained at the quark-model scale. In the chiral quark models in the chiral limit, one has at $t = 0$ very simple expressions [15,21,28],

$$H^{I=1}(X, \xi, 0) = \theta(1 - X^2),$$
$$H^{I=0}(X, \xi, 0) = \theta((1 - X)(X - \xi)) - \theta((X + 1) \times (-\xi - X)), \tag{43}$$

where $\theta(x)$ is the Heaviside step function. It follows from the definition (18) that at the quark-model scale the following relations hold [55],

$$A_{2j+1,2i}(0) = \begin{cases} \frac{1}{2j+1} & \text{for } i = 0 \\ 0 & \text{otherwise,} \end{cases}$$
$$A_{2j+2,2i}(0) = \begin{cases} \frac{1}{2j+2} & \text{for } i = 0 \\ -\frac{1}{2j+2} & \text{for } i = j+1 \\ 0 & \text{otherwise} \end{cases} \tag{44}$$

(quark-model scale).

These relations can be seen in Fig. 4(a). The form factors tend to zero very slowly at large $-t$.

Another property follows from the fact that in the considered model $H^{I=0}(X, 1, t) = 0$ for any value of t. Then Eq. (18) yields [55]

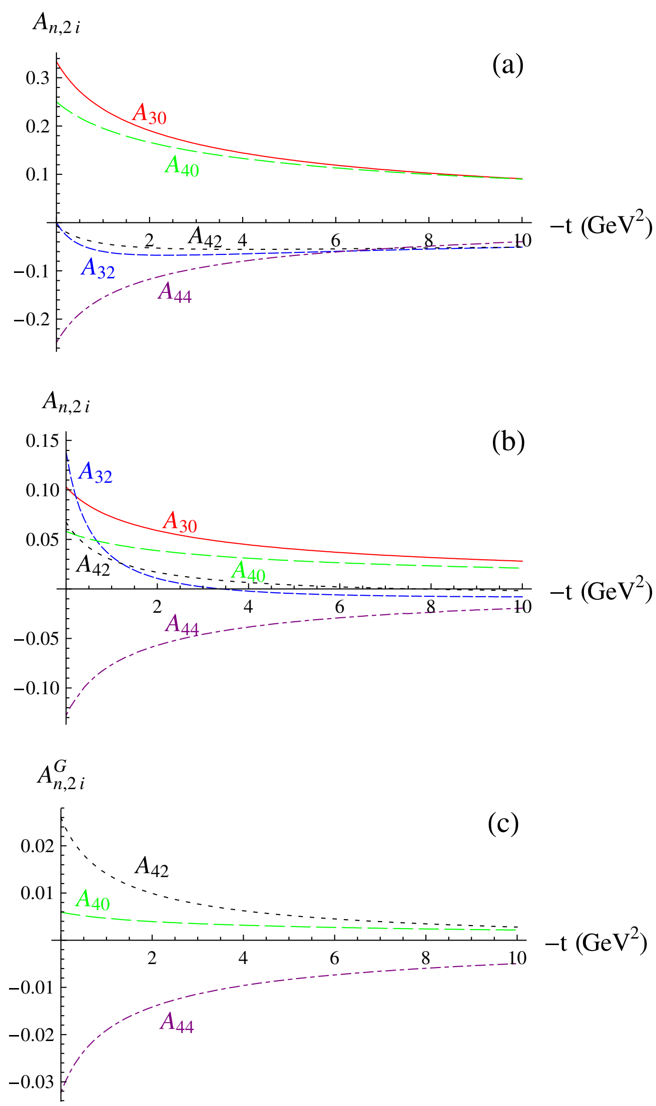

FIG. 4 (color online). Generalized form factors $A_{3,2i}$ and $A_{4,2i}$ of the pion in the SQM at the quark-model scale Q_0 (a) and at the lattice scale $Q = 2$ GeV (b), and the gluon form factors $A^G_{4,2i}$ at $Q = 2$ GeV (c).

$$\sum_{i=0}^{j+1} A_{2j+2,2i}(t) = 0. \quad (45)$$

This feature can be seen in Fig. 4(c).

While the lowest-order form factors, i.e. electromagnetic and gravitational, do not evolve with the running scale Q, the higher-order form factors change when we pass from the reference quark-model scale Q_0 to Q. Our analysis proceeds as follows: We carry out the leading-order DGLAP-Efremov-Radyuskin-Brodsky-Lepage (ERBL) evolution for the quark-model GPDs from the quark-model scale

$$Q_0 = 0.31 \text{ GeV} \quad (46)$$

to the scale of the lattice calculation, $Q = 2$ GeV. Note that the GPDs at the quark-model scale do not exhibit factorization in the t variable. In fact, this is the reason for the nontrivial change of the higher-order form factors with the scale. After the evolution we take the moments (18) at several values of ξ and then disentangle the generalized form factors via solving a set of linear equations. For the LO ERBL DGLAP evolution we use the method and the numerical program of Ref. [80]. The result of our calculations is presented in Fig. 4(b). We notice a dramatic change, both in the value at $t = 0$ and in the shape of the form factors compared to the behavior of Fig. 4(a) at the quark-model scale.

Formally, as $Q^2 \to \infty$ the GPDs approach their asymptotic forms contained entirely in the ERBL region $|X| < \xi$. Explicitly, we have in this limit[15]

$$\begin{aligned} H^{I=1} &= \frac{3}{2\xi}\left(1 - \frac{X^2}{\xi^2}\right)F_V(t), \\ H^{I=0} &= (1-\xi^2)\frac{15}{4\xi^2}\frac{N_f}{4C_F + N_f}\frac{X}{\xi}\left(1 - \frac{X^2}{\xi^2}\right)\Theta(t), \\ XH^G &= (1-\xi^2)\frac{15}{4\xi}\frac{C_F}{4C_F + N_f}\left(1 - \frac{X^2}{\xi^2}\right)^2\Theta(t) \\ &(Q^2 \to \infty) \end{aligned} \quad (47)$$

where $C_F = (N_c^2 - 1)/(2N_c)$ and $N_f = 3$. The proportionality factors follow from the normalization at the initial quark-model scale Q_0, as the charge- and momentum-conservation sum rules are invariants of the evolution,

$$\begin{aligned} &\int_{-1}^{1} dX H^{I=1}(X, \xi, t, Q^2) \\ &\quad = 2F_V(t), \\ &\int_{-1}^{1} dX[XH^{I=0}(X, \xi, t, Q^2) + XH_g(X, \xi, t, Q^2)] \\ &\quad = (1-\xi^2)\Theta(t), \end{aligned} \quad (48)$$

in accordance with Eqs. (19) and (20).

Evaluation of moments in Eq. (47) yields immediately

$$\begin{aligned} A_{2j+1,2i}(t) &= \begin{cases} \frac{3}{4j(j+2)+3}F_V(t) & \text{for } i = j \\ 0 & \text{otherwise,} \end{cases} \\ A_{2j+2,2i}(t) &= \begin{cases} \frac{N_f}{4C_F+N_f}\frac{15}{2[4j(j+4)+15]}\Theta(t) & \text{for } i = j \\ -A_{2j+2,2j}(t) & \text{for } i = j+1 \\ 0 & \text{otherwise,} \end{cases} \\ A^G_{2j+2,2i}(t) &= \frac{4C_f}{N_f}\frac{1}{2j+1}A_{2j+2,2i}(t) \qquad (Q^2 \to \infty). \end{aligned} \quad (49)$$

We note a qualitative difference of the asymptotic form factors compared to the form factors at the quark-model scale shown in Fig. 4. For the isovector case ($n = 2j + 1$) only the highest form factor, with $i = j$, does not vanish, while for the isoscalar case ($n = 2j + 2$) only the two highest moments, with $i = j + 1$ and $i = j$, are nonzero. The remaining moments tend to zero. This result is a prompt conclusion from the asymptotic forms (47). Note that in contrast to this behavior, at the quark-model scale all generalized form factors are nonzero. As mentioned previously, the form factors A_{10}, A_{20}, and A_{22} are invariants of the evolution. The asymptotic gluon form factors in Eq. (49) are related to the isoscalar quark form factors in a simple manner. Asymptotically, all generalized form factors become proportional to $F_V(t)$ or $\Theta(t)$ in the isovector and isoscalar channels, respectively.

Finally, we compare our values of the higher-order form factors at $t = 0$ to the lattice data provided in Sec. 7 of Ref. [3]. With the notation for the moments at $t = 0$,

$$\langle x^n \rangle = A_{n+1,0}(0), \quad (50)$$

one finds at the lattice scale of $Q = 2$ GeV

$$\begin{aligned} &\langle x \rangle = 0.271 \pm 0.016, \qquad \langle x^2 \rangle = 0.128 \pm 0.018, \\ &\langle x^3 \rangle = 0.074 \pm 0.027 \qquad \text{(lattice),} \end{aligned} \quad (51)$$

while in both chiral quark models we obtain, after the LO DGLAP evolution to the lattice scale,

$$\begin{aligned} &\langle x \rangle = 0.28 \pm 0.02, \qquad \langle x^2 \rangle = 0.10 \pm 0.02, \\ &\langle x^3 \rangle = 0.06 \pm 0.01 \qquad \text{(chiral quark models),} \end{aligned} \quad (52)$$

where the error bars come from the uncertainty of the scale Q_0 in Eq. (40). The two sets of numbers overlap within the error bars. This result is quite remarkable, as it shows that the hierarchy of the form factors at $t = 0$ found in full-QCD lattice calculations is properly reproduced in chiral quark models. The above form factors are simply the moments of the PDF of the pion. We recall that the PDF itself in the chiral quark models reproduces very well the experimental [52] and transverse lattice data of Ref. [53]; see Figs. 8 and 9 of Ref. [15].

VII. CONCLUSIONS

Here are our main points:

(1) The gravitational form factor obtained from the spectral quark model in the chiral limit agrees very well with the lattice data of Refs. [2,3]. We have performed a global fit to the electromagnetic and the quark part of the gravitational form factors and obtained very reasonable values for the evolution ratio and the vector-meson mass. The longer range of the gravitational form factor follows from a different analytic expression compared to the electromagnetic form factor.

(2) The NJL model does not provide such an excellent agreement, although the qualitative features are very similar to the SQM.

(3) We provide analytic expressions for the lowest-order form factors in both considered models. For the considered models in the chiral limit we find an explicit relation between the gravitational and vector form factors. In particular, the relation shows that in our case both gravitational form factors are equal, and that the mean squared electromagnetic radius is twice the gravitational one.

(4) The electromagnetic and gravitational form factors do not evolve with the scale, but the higher-order generalized form factors do. We have performed the leading-order ERBL DGLAP QCD evolution of the pion GPDs and obtained via moments the generalized form factors at the scale of the lattice measurements.

(5) The generalized form factors at $t = 0$ found in full-QCD lattice simulations are reproduced in chiral quark models within the error bars corresponding to statistical and model uncertainties.

(6) Our predictions can be further tested with future lattice simulations for higher-order form factors. The behavior is nontrivial, with form factors having different signs, magnitude, and asymptotic falloff.

(7) Lattice simulations for the gluon form factors would provide very useful independent information, which could be used to verify the model predictions.

ACKNOWLEDGMENTS

The authors are grateful to Dirk Brömmel for helpful email exchanges and for providing the lattice data of Refs. [3] for our figures; the authors also cordially thank Krzysztof Golec-Biernat for making available his computer code for solving the QCD evolution equations for the GPDs. This work was supported by Polish Ministry of Science and Higher Education, Grant No. N202 034 32/0918 and No. N202 249235; Spanish DGI and FEDER funds through Grant No. FIS2005-00810; Junta de Andalucía Grant No. FQM225-05; and EU Integrated Infrastructure Initiative Hadron Physics Project Contract No. RII3-CT-2004-506078.

APPENDIX: RELATION BETWEEN GRAVITATIONAL AND ELECTROMAGNETIC FORM FACTORS

In this appendix we show an explicit calculation of form factors in the SQM and prove as a by-product the result of Eq. (31). The proof also applies to the NJL model with the PV regularization, as that model can also be written in terms of the spectral representation (see below).

The SQM is defined by the generalized Lehman representation of the quark propagator

$$S(\not p)\int_C d\omega \frac{\rho(\omega)}{\not p - \omega}. \tag{A1}$$

The method exploited in Ref. [4] was mainly based on writing down Ward identities for the corresponding vertex functions at the quark level, and then closing the quark line to make one-loop calculations. As discussed in later works (see e.g. [62,68]) this is fully equivalent to proceeding directly through the effective action which we sketch now. Using the action of Eq. (22) one can compute the energy-momentum tensor as a functional derivative of the action with respect to an external space-time-dependent metric, $g_{\mu\nu}(x)$, around the flat space-time metric $\eta_{\mu\nu}$ [we take the signature $(+---)$],

$$\begin{aligned}\frac{1}{2}\Theta^{\mu\nu}(x) &= \frac{\delta\Gamma}{\delta g_{\mu\nu}(x)}\Big|_{g_{\mu\nu}=\eta_{\mu\nu}} \\ &= -\mathrm{i}\frac{N_c}{2}\int_C d\omega\rho(\omega) \\ &\quad\times\langle x|\{O^{\mu\nu},(i\not\partial-\omega U^5)^{-1}\}|x\rangle,\end{aligned} \tag{A2}$$

where

$$O^{\mu\nu} = \frac{\mathrm{i}}{2}(\gamma^\mu\partial^\nu + \gamma^\nu\partial^\mu) - g^{\mu\nu}(\mathrm{i}\not\partial - \omega), \tag{A3}$$

and $U^5 = \exp(i\gamma_5\boldsymbol{\tau}\cdot\boldsymbol{\phi}/f)$ with $\boldsymbol{\phi}$ the pion field in the nonlinear realization. For the calculation of the gravitational form factor, we expand up to second order in the pion field, corresponding to evaluating the diagrams of Fig. 1. In the Cartesian isospin basis one has

$$\begin{aligned}\langle\pi^b|\Theta_{\mu\nu}|\pi^a\rangle &= -N_c\int d\omega\rho(\omega)\int\frac{d^4k}{(2\pi)^4}\mathrm{Tr}\Big\{\Theta_{\mu\nu}(k+q,k) \\ &\quad\times\Big[\frac{i}{\not k-\omega}\Big(-\frac{\tau_a\gamma_5\omega}{f}\Big)\frac{i}{\not k-\not p-\omega} \\ &\quad\times\Big(-\frac{\tau_b\gamma_5\omega}{f}\Big)\frac{i}{\not k+\not q-\omega}+\frac{i}{\not k-\omega}\frac{i\delta_{ab}\omega}{2f^2} \\ &\quad\times\frac{i}{\not k+\not q-\omega}\Big]+\text{crossed}\Big\},\end{aligned} \tag{A4}$$

where the quark gravitational vertex is given by

$$\begin{aligned}\Theta_{\mu\nu}(k+q,k) &= \tfrac{1}{4}[(2k_\mu+q_\mu)\gamma_\nu+(2k_\nu+q_\nu)\gamma_\mu] \\ &\quad-\tfrac{1}{2}g_{\mu\nu}(2\not k+\not q-\omega).\end{aligned} \tag{A5}$$

After computing the traces and using the Feynman trick in the integrals, in the chiral limit the result is

$$\Theta_1(q^2) = \frac{N_c}{4\pi^2 f^2}\int d\omega\rho(\omega)\omega^2 \int_0^1 \frac{dx}{x(1-x)q^2} \times [-\omega^2\log\omega^2 + x(1-x)q^2 + (\omega^2 - x(1-x)q^2)\log(\omega^2 - x(1-x)q^2)],$$
$$\Theta_2(q^2) = \Theta_1(q^2). \quad (A6)$$

In the low-momentum limit we may use Eq. (5) as deduced from χPT in the presence of gravity [61] to get

$$L_{11} = \frac{N_c}{192\pi^2}, \quad (A7)$$

$$L_{12} = -\frac{N_c}{96\pi^2}, \quad (A8)$$

$$L_{13} = -\frac{N_c}{(4\pi)^2}\frac{\rho_1{}'}{12B_0} = \frac{f^2}{24M_S^2}, \quad (A9)$$

in agreement with the derivative expansion of the SQM [62].

Proceeding similarly with the vector form factor, we get

$$\langle\pi^a|J_V^{\mu,b}|\pi^c\rangle = -N_c\int d\omega\rho(\omega)\int\frac{d^4k}{(2\pi)^4}\mathrm{Tr}\Big[\gamma_\mu\frac{\tau_b}{2} \times \frac{i}{\not k - \omega}\Big(-\frac{\tau_c\gamma_5\omega}{f}\Big)\frac{i}{\not p + \not k - \omega} \times\Big(-\frac{\tau_a\gamma_5\omega}{f}\Big)\frac{i}{\not q - \not k - \omega}\Big]. \quad (A10)$$

For on-shell massless pions the electromagnetic form factor reads

$$F_V(q^2) = -\frac{N_c}{4\pi^2 f^2}\int d\omega\rho(\omega)\omega^2 \times\int_0^1 dx\log[\omega^2 - x(1-x)q^2]. \quad (A11)$$

Charge normalization, $F_V(0) = 1$, and energy-momentum normalization, $\Theta_2(0) = 1$, imply

$$1 = F_V(0) = \Theta_2(0) = -\frac{N_c}{4\pi^2 f^2}\int d\omega\rho(\omega)\omega^2\log\omega^2 = \frac{N_c m_\rho^2}{24\pi^2 f^2}, \quad (A12)$$

where in the second line the vector-meson realization, Eq. (23), has been used. The value agrees with the value of the pion weak decay constant obtained from the corresponding axial matrix element [4].

With the representations of Eqs. (A6) and (A11) the result in Eq. (31) can be readily derived, without any reference to the specific realization given by Eq. (23).

The above proof also holds for the NJL model in the PV regularization. This class of models can be cast explicitly in the spectral-representation form, using $\rho(\omega) = \delta(\omega - M) + \Sigma_i c_i\delta(\omega - \sqrt{M^2 + \Lambda_i^2})$, where c_i and Λ_i are the PV constants. Then all the above algebraic steps carry over, and the result (31) holds for the NJL model with PV regularization as well.

[1] H. Pagels, Phys. Rev. **144**, 1250 (1966).
[2] D. Brommel *et al.*, Proc. Sci., LAT2005 (2006) 360 [arXiv:hep-lat/0509133].
[3] D. Brommel, Ph.D. thesis, University of Regensburg, Regensburg, Germany [DESY Report No. DESY-THESIS-2007-023, 2007].
[4] E. Ruiz Arriola and W. Broniowski, Phys. Rev. D **67**, 074021 (2003).
[5] X.-D. Ji, J. Phys. G **24**, 1181 (1998).
[6] A. V. Radyushkin, arXiv:hep-ph/0101225.
[7] K. Goeke, M. V. Polyakov, and M. Vanderhaeghen, Prog. Part. Nucl. Phys. **47**, 401 (2001).
[8] A. P. Bakulev, R. Ruskov, K. Goeke, and N. G. Stefanis, Phys. Rev. D **62**, 054018 (2000).
[9] M. Diehl, Phys. Rep. **388**, 41 (2003).
[10] X.-D. Ji, Annu. Rev. Nucl. Part. Sci. **54**, 413 (2004).
[11] A. V. Belitsky and A. V. Radyushkin, Phys. Rep. **418**, 1 (2005).
[12] T. Feldmann, Eur. Phys. J. Special Topics **140**, 135 (2007).
[13] S. Boffi and B. Pasquini, Riv. Nuovo Cim. **30**, 387 (2007).
[14] D. Amrath, M. Diehl, and J.-P. Lansberg, arXiv:0807.4474.
[15] W. Broniowski, E. R. Arriola, and K. Golec-Biernat, Phys. Rev. D **77**, 034023 (2008).
[16] R. M. Davidson and E. Ruiz Arriola, Phys. Lett. B **348**, 163 (1995).
[17] E. Ruiz Arriola, arXiv:hep-ph/0107087.
[18] R. M. Davidson and E. Ruiz Arriola, Acta Phys. Pol. B **33**, 1791 (2002).
[19] W. Broniowski and E. Ruiz Arriola, Phys. Lett. B **574**, 57 (2003).
[20] A. E. Dorokhov and L. Tomio, arXiv:hep-ph/9803329.
[21] M. V. Polyakov and C. Weiss, Phys. Rev. D **60**, 114017 (1999).
[22] A. E. Dorokhov and L. Tomio, Phys. Rev. D **62**, 014016 (2000).
[23] I. V. Anikin, A. E. Dorokhov, A. E. Maksimov, L. Tomio, and V. Vento, Nucl. Phys. **A678**, 175 (2000).
[24] I. V. Anikin, A. E. Dorokhov, A. E. Maksimov, and L. Tomio, Phys. At. Nucl. **63**, 489 (2000).

[25] M. Praszalowicz and A. Rostworowski, arXiv:hep-ph/0205177.
[26] M. Praszalowicz and A. Rostworowski, Acta Phys. Pol. B **34**, 2699 (2003).
[27] A. Bzdak and M. Praszalowicz, Acta Phys. Pol. B **34**, 3401 (2003).
[28] L. Theussl, S. Noguera, and V. Vento, Eur. Phys. J. A **20**, 483 (2004).
[29] F. Bissey, J. R. Cudell, J. Cugnon, J. P. Lansberg, and P. Stassart, Phys. Lett. B **587**, 189 (2004).
[30] S. Noguera and V. Vento, Eur. Phys. J. A **28**, 227 (2006).
[31] B. C. Tiburzi and G. A. Miller, Phys. Rev. D **67**, 013010 (2003).
[32] B. C. Tiburzi and G. A. Miller, Phys. Rev. D **67**, 113004 (2003).
[33] A. V. Radyushkin, Phys. Lett. B **449**, 81 (1999).
[34] B. Pire, J. Soffer, and O. Teryaev, Eur. Phys. J. C **8**, 103 (1999).
[35] P. V. Pobylitsa, Phys. Rev. D **65**, 077504 (2002).
[36] M. V. Polyakov, Nucl. Phys. **B555**, 231 (1999).
[37] I. V. Anikin, A. E. Dorokhov, and L. Tomio, Phys. Lett. B **475**, 361 (2000).
[38] M. Praszalowicz and A. Rostworowski, Phys. Rev. D **64**, 074003 (2001).
[39] A. E. Dorokhov, JETP Lett. **77**, 63 (2003).
[40] E. Ruiz Arriola and W. Broniowski, Phys. Rev. D **66**, 094016 (2002).
[41] E. Ruiz Arriola, Acta Phys. Pol. B **33**, 4443 (2002).
[42] A. P. Bakulev, S. V. Mikhailov, A. V. Pimikov, and N. G. Stefanis, Fiz. B **17**, 217 (2008).
[43] B. Pire and L. Szymanowski, Phys. Rev. D **71**, 111501 (2005).
[44] B. Pire and L. Szymanowski, Phys. Lett. B **622**, 83 (2005).
[45] J. P. Lansberg, B. Pire, and L. Szymanowski, Phys. Rev. D **73**, 074014 (2006).
[46] J. P. Lansberg, B. Pire, and L. Szymanowski, *Exclusive Reactions at High Momentum Transfer* (World Scientific, Singapore, 2008), p. 367.
[47] B. C. Tiburzi, Phys. Rev. D **72**, 094001 (2005).
[48] W. Broniowski and E. R. Arriola, Phys. Lett. B **649**, 49 (2007).
[49] A. Courtoy and S. Noguera, Phys. Rev. D **76**, 094026 (2007).
[50] A. Courtoy and S. Noguera, Prog. Part. Nucl. Phys. **61**, 170 (2008).
[51] P. Kotko and M. Praszalowicz, arXiv:0803.2847.
[52] J. S. Conway *et al.*, Phys. Rev. D **39**, 92 (1989).
[53] S. Dalley and B. van de Sande, Phys. Rev. D **67**, 114507 (2003).
[54] E. M. Aitala *et al.* (E791), Phys. Rev. Lett. **86**, 4768 (2001).
[55] W. Broniowski, arXiv:0805.4589.
[56] J. Gasser and H. Leutwyler, Ann. Phys. (N.Y.) **158**, 142 (1984).
[57] J. Gasser and H. Leutwyler, Nucl. Phys. **B250**, 465 (1985).
[58] J. Gasser and H. Leutwyler, Nucl. Phys. **B250**, 517 (1985).
[59] A. Pich, Rep. Prog. Phys. **58**, 563 (1995).
[60] M. Diehl, A. Manashov, and A. Schafer, Phys. Lett. B **622**, 69 (2005).
[61] J. F. Donoghue and H. Leutwyler, Z. Phys. C **52**, 343 (1991).
[62] E. Megias, E. Ruiz Arriola, L. L. Salcedo, and W. Broniowski, Phys. Rev. D **70**, 034031 (2004).
[63] E. Megias, E. Ruiz Arriola, and L. L. Salcedo, Phys. Rev. D **72**, 014001 (2005).
[64] E. Ruiz Arriola, Phys. Lett. B **253**, 430 (1991).
[65] C. Schuren, E. Ruiz Arriola, and K. Goeke, Nucl. Phys. **A547**, 612 (1992).
[66] G. V. Efimov and M. A. Ivanov, *The Quark Confinement Model of Hadrons* (IOP Publishing, Bristol, UK, 1993).
[67] E. Ruiz Arriola and W. Broniowski, arXiv:hep-ph/0310044.
[68] E. R. Arriola, W. Broniowski, and B. Golli, Phys. Rev. D **76**, 014008 (2007).
[69] A. E. Dorokhov, W. Broniowski, and E. Ruiz Arriola, Phys. Rev. D **74**, 054023 (2006).
[70] H. Weigel, E. Ruiz Arriola, and L. P. Gamberg, Nucl. Phys. **B560**, 383 (1999).
[71] D. V. Shirkov and I. L. Solovtsov, Phys. Rev. Lett. **79**, 1209 (1997).
[72] N. G. Stefanis, W. Schroers, and H.-C. Kim, Eur. Phys. J. C **18**, 137 (2000).
[73] A. P. Bakulev, K. Passek-Kumericki, W. Schroers, and N. G. Stefanis, Phys. Rev. D **70**, 033014 (2004).
[74] A. P. Bakulev, A. I. Karanikas, and N. G. Stefanis, Phys. Rev. D **72**, 074015 (2005).
[75] J. Volmer *et al.* (Jefferson Lab F(pi)), Phys. Rev. Lett. **86**, 1713 (2001).
[76] V. Tadevosyan *et al.* (Jefferson Lab F(pi)), Phys. Rev. C **75**, 055205 (2007).
[77] T. Horn *et al.* (Jefferson Lab F(pi)-2), Phys. Rev. Lett. **97**, 192001 (2006).
[78] C. J. Bebek *et al.*, Phys. Rev. D **17**, 1693 (1978).
[79] A. Pich, arXiv:hep-ph/0205030.
[80] K. J. Golec-Biernat and A. D. Martin, Phys. Rev. D **59**, 014029 (1998).